JOURNAL OF MATERIALS SCIENCE 27 (1992) 351–357

Effects of ZrO_2 precursors on the synthesis of V–$ZrSiO_4$ solid solutions by the sol–gel method

G. MONRÓS, J. CARDA, M. A. TENA, P. ESCRIBANO
Department of Inorganic Chemistry, Colegio Universitario de Castellón, Spain
J. ALARCÓN
**Department of Inorganic Chemistry, Facultad de Ciencias Químicas, Universidad de Valencia, Spain Nave 2, 46003 Valencia, Apartado 224, Castellón, Spain*

The preparation of V–$ZrSiO_4$ solid solutions starting from different ZrO_2 precursors by using sol–gel methods is reported. The starting materials were hydrolysed and the dried gels were fired at a temperature between 500 and 900 °C with soaking times of 12 h. The organic character of zirconia precursors was stronger, i.e. the starting material had more carbon atoms, a higher temperature was necessary to make the first crystalline phase appear (ZrO_2(tetragonal)) and the temperature range for the whole phase transformation was narrower. In all dried gel samples the presence of infrared bands which might be associated with either Si–O–Zr or Si–O–V was not observed. On the other hand, some bands could be attributed to a silica network and ZrO_8 groups. The main steps in V–$ZrSiO_4$ solid solutions were confirmed. ZrO_2(tetragonal) is crystallized on heating from an amorphous sample. The ZrO_2(tetragonal) → ZrO_2(monoclinic) phase transformation then occurs and immediately afterwards the zircon formation begins. Finer textures in samples were obtained from polymeric gels rather than for colloidal gel samples, as seen from the scanning electron micrographs.

1. Introduction

The preparation of solid solutions by the conventional ceramic method presents some drawbacks. Thus, it is difficult to obtain mixtures with high homogeneity which allows higher reaction grades to be reached at low temperatures. Likewise, the necessary high temperatures produce the loss of volatile reactives and consequently the deviation of the systems initial stoichiometric condition. In previous works [1, 2] sol–gel techniques were used in the preparation of solid solutions, to produce a gel in which the particle size and the degree of high homogeneity allow a significant increase in the efficiency of the process at lower temperatures. It was observed that one of the steps in the formation mechanism of doped zircon was the ZrO_2(tetragonal) → ZrO_2(monoclinic) phase transformation. The particle size and morphology of ZrO_2, including the microstructure of the whole system, strongly influences the transformation temperature [3, 4]. Our purpose in the present study was to investigate the effects of the different zirconium starting materials with increasing organic character on the zircon formation. Gels of composition $(ZrO_2)_{0.9}\cdot(SiO_2)\cdot(V_2O_5)_{0.05}$ were prepared. This composition was chosen because, as in previous studies, it was detected to be adequate to optimize the synthesis process. The gels were submitted to different thermal treatments and subsequent characterization by different techniques. The results obtained are reported here and they are compared with those obtained from a colloidal gel.

One further objective was to check the steps of the zircon formation mechanism followed by the prepared samples.

2. Experimental procedure

2.1. Preparation of gels

The starting materials used were NH_4VO_3, vanadium(IV) oxide acetylacetonate, zirconium(IV) acetate (industrial quality), zirconium(IV) propionate (industrial quality), zirconium(IV) propoxide (industrial quality), $ZrOCl_2\cdot 6H_2O$, tetraethyl orthosilicate (TEOS) and colloidal silica (industrial quality) in water or absolute alcohol media depending on the method. The starting materials for each sample are given in Table I.

Sample 1 was prepared by a method described previously [1]. NH_4VO_3 was dissolved in 3 M HNO_3 (10 ml acid per 10 g end-product). This solution was added to a suspension of colloidal silica in 100 ml water. After a few minutes of vigorous stirring, a clear and stable suspension was obtained, to which the zirconium salt solution in 100 ml water was added. To the solution obtained at 70 °C with continuous stirring, a solution of ammonium hydroxide was added dropwise (pH = 5–6) until gellation occurred.

A solution of NH_4VO_3 in 3 M HNO_3 was mixed with a solution of a zirconium salt in ethanol for the preparation of Samples 2, 3 and 4. Then TEOS was added to the resultant mixture with constant stirring at 70 °C and refluxing for 24 h. The molar ratio

0022–2461/92 $03.00 + .12

TABLE I Characteristics of gels prepared with different starting materials in $(ZrO_2)_{0.9} \cdot SiO_2 \cdot (V_2O_5)_{0.05}$ composition

Sample	Starting materials[a]	Mixture solution	Wet gels	Dried gels
1	NH_4VO_3, ZrAc, colloidal SiO_2	yellow opaque	yellow homogeneous	yellow homogeneous
2	NH_4VO_3, $ZrOCl_2 \cdot 6H_2O$, TEOS	yellow transparent	green-yellow non homog.	black granulated
3	NH_4VO_3, ZrAc, TEOS	red transparent	green-yellow homogeneous	coffe homogeneous
4	NH_4VO_3, ZrPr, TEOS	red transparent	green-yellow homogeneous	coffe homogeneous
5	VO(oacac)2, n-prop Zr, TEOS	green transparent	coffe homogeneous	coffe homogeneous

[a] Materials: NH_4VO_3 and $ZrOCl_2 \cdot 6H_2O$ from Merck, colloidal silica is Aerosil 200 from Degussa, TEOS: tetraethyl orthosilicate from Merck, VO(oacac)2: vanadyl oxiacetylacetonate from Fluka, ZrAc: zirconium(IV) acetate, ZrPr: zirconium(IV) propionate from Aldabo-Julia, n-prop Zr: Zr(IV) n-propoxide from Fluka.

H_2O:TEOS used was 1:8. Water was added as 3 M HNO_3 solution. The dilution in the resultant solution was 1:13 as TEOS:alcohol molar ratio. The final solutions were homogeneous and translucent. In sample 2 gellation began prior to 4 h reaction, producing a green–yellow gel with some inhomogeneities after 17 h, with greener shades at the bottom and yellower at the top. Similarly, in Samples 3 and 4, gellation also began before 4 h; however, the gels obtained in these cases were more homogeneous than in Sample 2. Gel 2 was dried using an infrared lamp and the Gels 3 and 4 were allowed to dry at room temperature.

In Sample 5, a solution of 3 M HNO_3 and $VO(acac.)_2$ was added to TEOS solution in ethanol, keeping the molar ratios TEOS:H_2O = 1:0.8 and

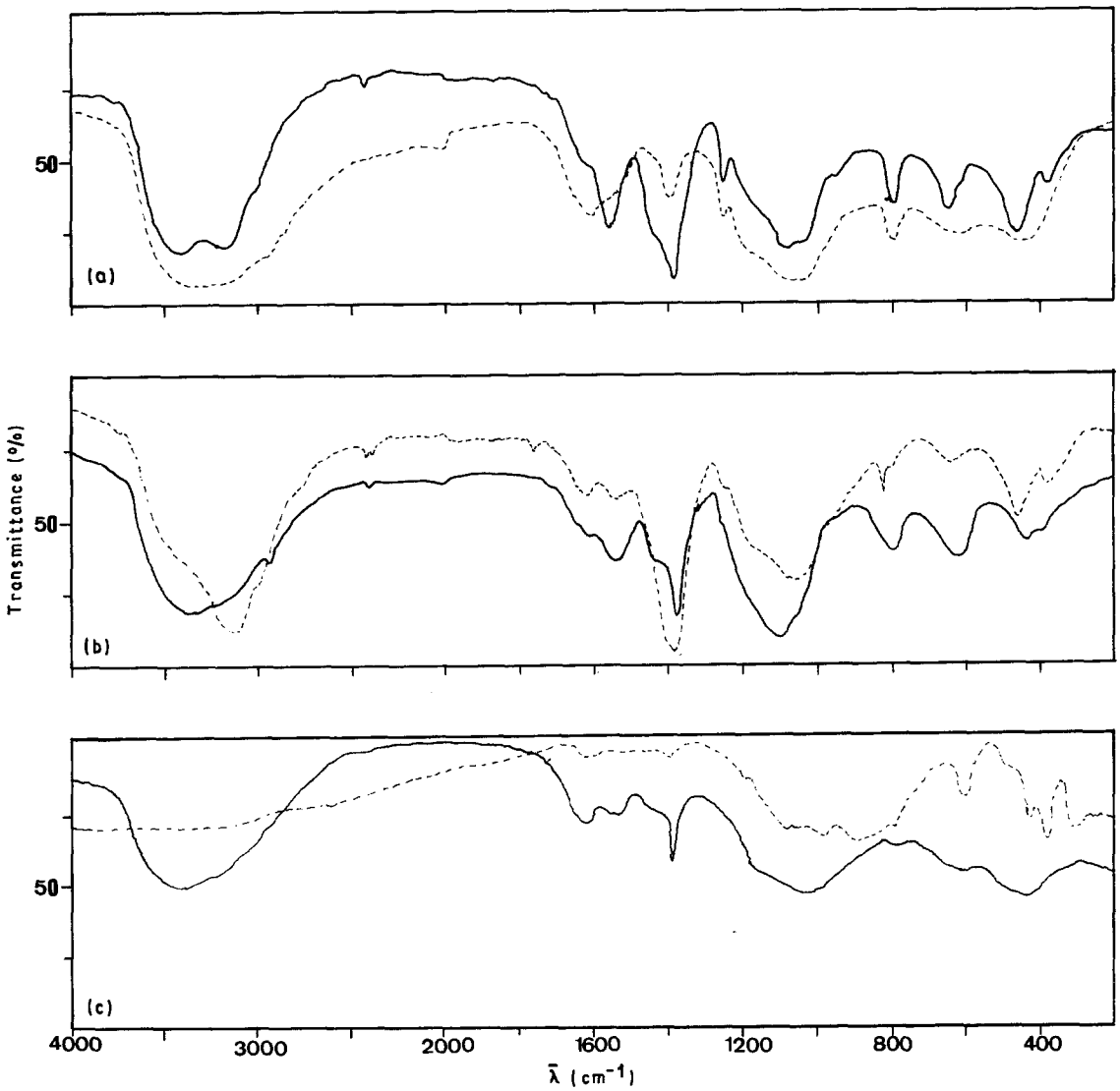

Figure 1 Infrared spectra of raw samples and Sample 5 fired at 1000 °C/12 h. (a) Raw samples, (—) 1, (– – –) 2; (b) raw samples, (——) 3, (– – –) 4; (c) (——) raw sample 5, (– – –) Sample 5 fired at 1000 °C.

TEOS: H^+ = 1:0.05. The dilution ratio used was the same as in Samples 2, 3 and 4. The solution obtained was refluxed at 70 °C with continuous stirring for 2 h, and changed from green to coffee colour. A stoichiometric amount of zirconium *n*-propoxide was added to the above solution and refluxed for 24 h with constant stirring. The beaker containing the solution was allowed to stand for several days under room temperature to allow drying to occur. Clear and very homogeneous coffee-coloured bulk gels were obtained.

2.2. Firing of samples

The gels were calcined in an electric kiln at a temperature between 500 and 900 °C with soaking times of 12 h.

2.3. Characterization of samples

Chemical and structural evolution of as-dried gels by thermal treatment was observed using several techniques.

Infrared transmission spectra were obtained in the range 4000–200 cm^{-1} using the KBr pellet technique with a Philips spectrometer.

Differential thermal analysis (DTA) and thermogravimetric analysis were carried out on a Mettler instrument in air, using a platinum crucible and a heating rate of 10 °C min^{-1}. Finely powdered alumina was used as reference substance.

X-ray diffraction (XRD) analysis was performed using a Philips X-ray diffractometer with Ni-filtered CuK_α radiation.

The texture of the thermally treated samples was determined by scanning electron microscopy (SEM) with a Philips microscope.

3. Results and discussion

3.1. Infrared spectroscopy of samples

Infrared spectra of raw samples and Sample 5 fired at 1000 °C/12 h are shown in Fig. 1. The data of the IR spectra of samples fired at different temperatures are summarized in Table II.

In raw gels, the bands at 3410 and 1522 cm^{-1} are associated with stretching vibrations of OH groups and molecular H_2O, respectively [3]. The bands at 1107, 790 and 457 cm^{-1} are all attributed to different vibration modes of Si–O–Si and O–Si–O. Thus, the first band localized at 1107 cm^{-1} is associated with stretching vibrations of the Si–O bond [4], the other two bands at 790 and 457 cm^{-1} are attributed to bending modes of Si–O–Si and O–Si–O.

The band at 645 cm^{-1} can be associated with zirconium–oxygen bonds in ZrO_8 groups. The bands localized at 1610, 950, 610 and 375 cm^{-1} are all associated with the V–O bond. The peaks at 1382 and

TABLE II Ir bands evolution with temperature (°C)

Sample	Bands	Raw	500	700	800	1000
1	OH	3410, 1552	3420		–	–
	Si–O	1107, 790, 457	1100, 800, 457		1100, 760	–
	Zr–O/ZrO_8	645	–		880, 611, 428	891, 610, 427
					375, 307	385, 312
	V–O	1610, 950, 610	1616		1630, 979	1629, 978
		375				
	NH_4^+	3164, 1382	3200, 1396		1397	–
	NO_3^-	1382, 821	1396		1397	–
2	O–H	3300, 1550				–
	Si–O	1075, 800, 450				1080, 440
	Zr–O/ZrO_8	625				900, 620, 420
						380, 310
	V–O	1620, 975				–
	NO_3^-	1400				–
3	O–H	3400, 1530		3400		
	Si–O	1100, 800, 440		1100, 900		
				800, 425		idem 2/1000 °C
	Zr–O/ZrO_8	625		600		
	V–O	1610, 950		–		
	NO_3^-	1380		–		
4	O–H	3400, 1525		3420, 1630		
	Si–O	1120, 800, 425		1100, 800		
				460		idem 2/1000 °C
	Zr–O/ZrO_8	620		610		
	V–O	630, 975		–		
	NO_3^-	1375		–		
5	O–H	3393, 1527	3450		–	–
	Si–O	1021, 776, 435	1004, 435		990, 776	1062
	Zr–O/ZrO_8	599	–		881, 605, 428	900, 603, 429
					376, 301	382, 312
	V–O	1618, 375	1617		–	1617, 979
	NO_3^-	1383	1399		–	–

821 cm^{-1} are assigned to NO_3^- [5], and are seen to disappear as the firing temperature increases. However, in Sample 1, from colloidal gels, these peaks appear even after firing at 800 °C. Similarly, in Sample 1 bands appear at 3164 and 1382 cm^{-1} associated with NH_4^+ groups [6].

In general, all the bands previously indicated display a small shift. In the case of peaks of the ZrO_8 group the shifting is particularly important (645 cm^{-1} for Sample 1 and 600 cm^{-1} for Sample 5). The bands associated with OH groups and H_2O decrease with increasing firing temperature of samples, because physically absorbed water and bonded hydroxyl groups are lost.

The bands attributed to V–O bonds gradually disappear to increase, thus increasing the organic nature of the gel.

When the zircon crystalline phase is detected, bands at 900, 620, 420, 380 and 310 cm^{-1}, together with others of lower intensity associated with Si–O and V–O bonds, are obtained.

3.2. Thermal analysis

DTA, TGA and DTG curves of dried samples are shown in Figs 2 and 3. In polymeric gel samples the DTA curves for all samples display some common features. Similarly, in the TGA curves, weight losses are shown to begin with the first endothermic peak and to end within the range of the first exothermic peak. The DTA curves of Samples 2–5 exhibit an endothermic peak at 120–250 °C. In the same temperature range, a weight loss is detected in TGA curves, which could be ascribed to the evaporation of residual water and organic solvent entrapped in micropores of the gel.

In the temperature range 300–450 °C, a high exothermic peak is observed in Samples 2, 4 and 5. Also, in this temperature region, TGA shows a weight loss in these samples, indicating that it can be ascribed to the oxidation of organics. In addition, two exothermic peaks are observed at 300 and 440 °C for Sample 3 with an associated change in the slope of the TGA curve, reflected in the DTG curve, which can be

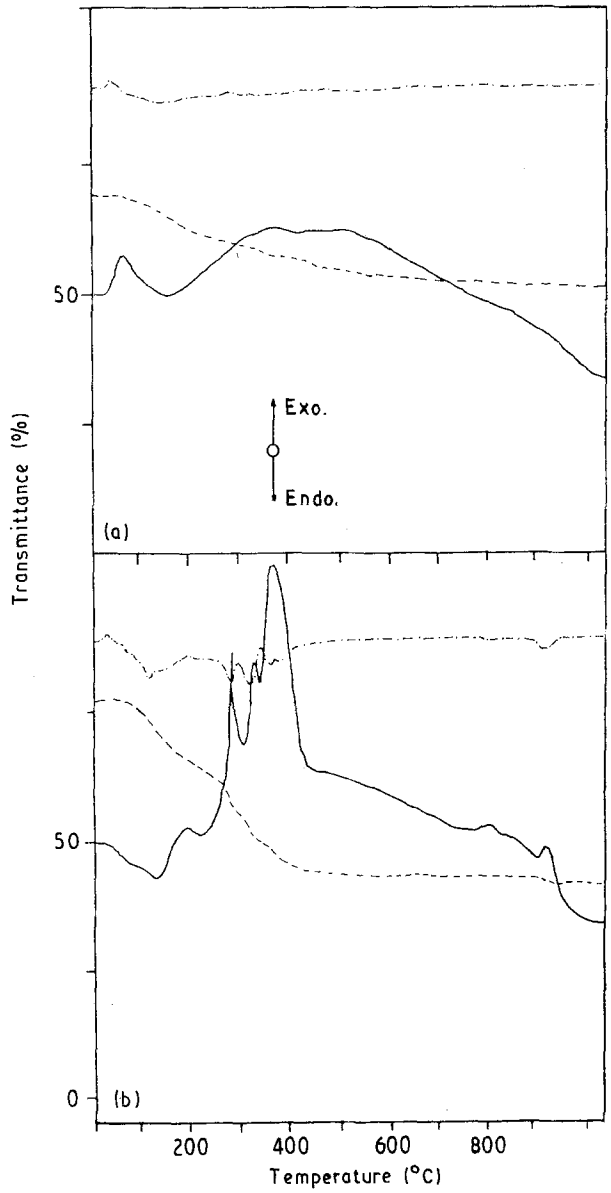

Figure 2 (—) DTA, (– – –) TGA and (–.–) DTG analysis of Samples (a) 2 and (b) 3 in air using a Pt crucible and a heating rate of 10 °C min^{-1}.

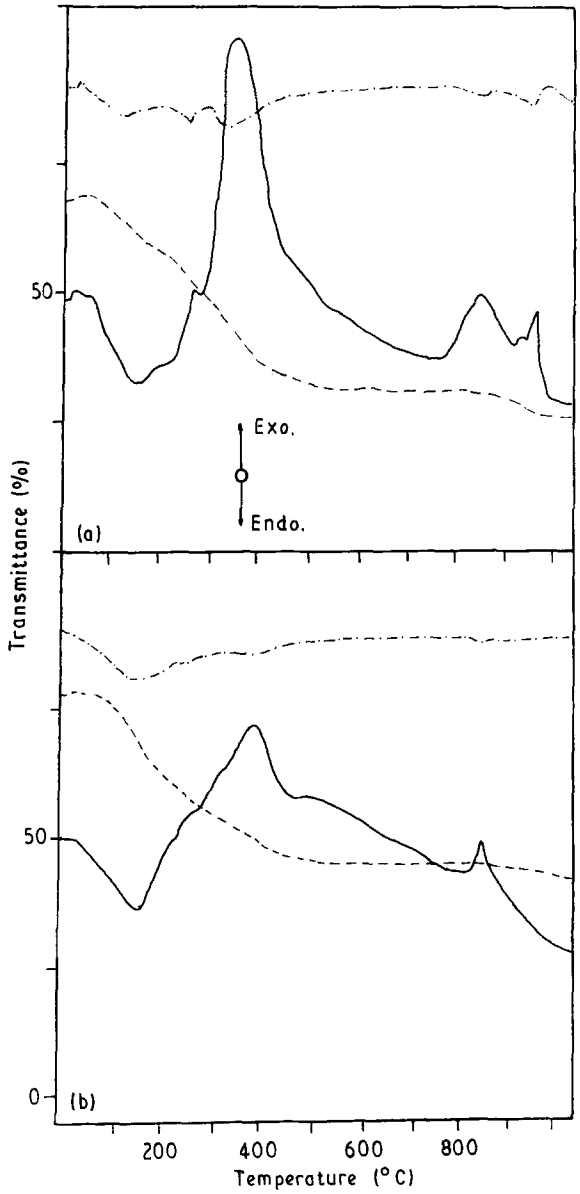

Figure 3 (—) DTA, (– – –) TGA and (—.—) DTG analysis of Samples (a) 4 and (b) 5 in air using a Pt crucible and a heating rate of 10 °C min^{-1}.

associated with the decomposition of acetate groups [7]. The second exothermic peak at 800 °C in Samples 3–5 with no associated weight loss in the TGA curves can be ascribed to crystallization of ZrO_2 (tetragonal). In addition, a third exothermic peak is shown in Samples 3 and 4 which can be assigned to the formation of $ZrSiO_4$.

3.3. X-ray diffraction

The evolution of the crystalline phases detected at different temperatures is summarized in Table III. The X-ray diffractograms for all samples fired at 750 °C/12 h are shown in Fig. 4; the diffractogram of Sample 1 is obtained at twice the scale of the others.

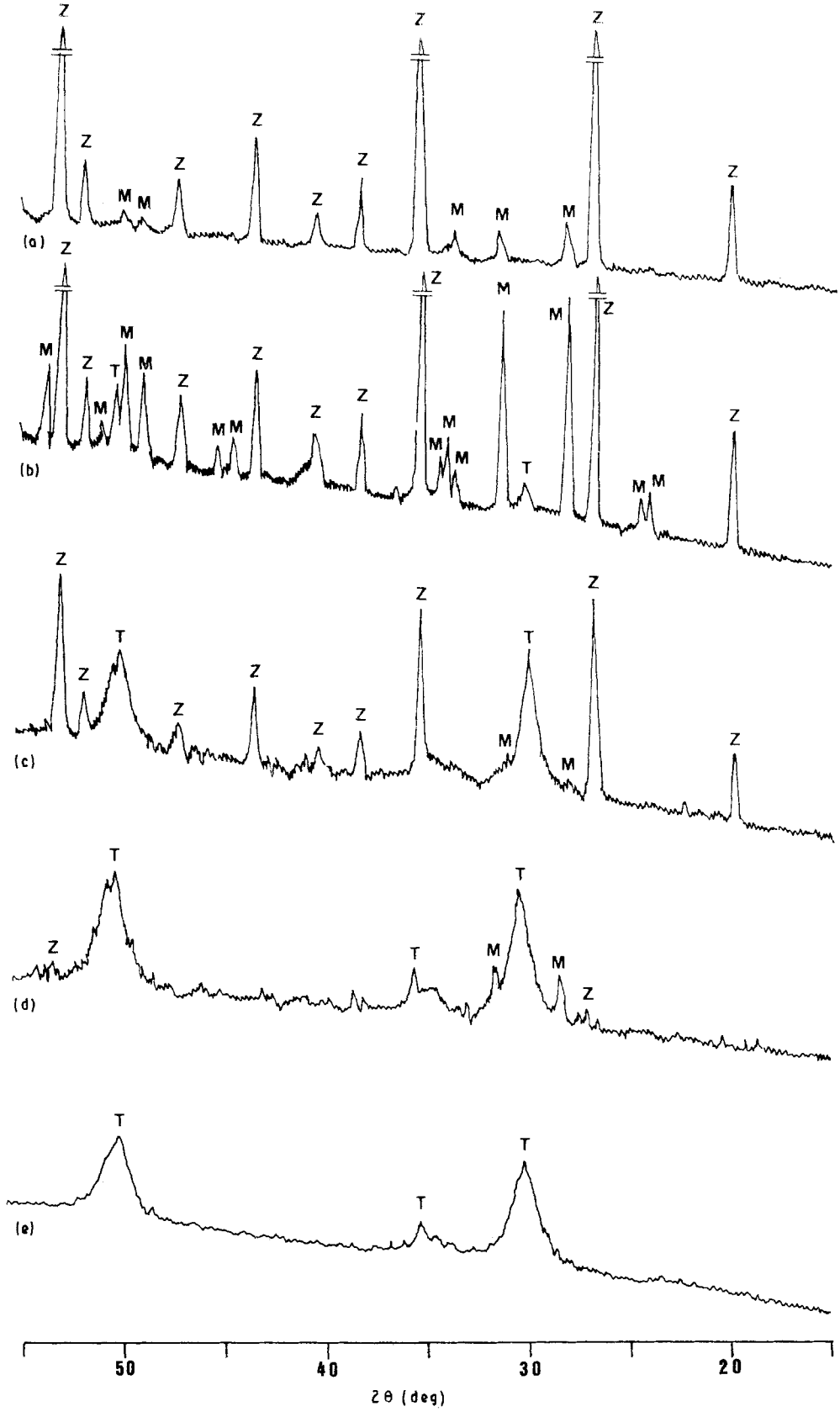

Figure 4 X-ray diffractograms of samples fired at 750 °C/12 h. The scale of the diffractogram from Sample 1 is twice that of the others. Samples (a) 1, (b) 2, (c) 3, (d) 4, (e) 5.

TABLE III X-ray phases detected in function of firing temperature

Sample	Firing temperature (°C)					
	500	600	700	750	800	900
1	T(m)	T(m), M(w)	Z(m), M(m), T(m)	Z(s), M(m)	Z(s), M(w)	Z(s), M(vw), C(vw)
2	T(m)	T(m)	T(m), M(vw)	Z(s), M(m), T(w)	Z(s), M(vw), C(vw)	Z(s), C(vw)
3	A	A	Z(vw)	Z(m), T(m), M(vw)	Z(s)	Z(s), C(vw)
4	A	A	T(w)	Z(vw), T(m), M(w)	Z(s)	Z(s), C(vw)
5	A	A	A	T(m)	Z(m), M(w)	Z(s), C(w)

Crystalline phases: T (ZrO_2 tetragonal), M (ZrO_2 monoclinic), Z ($ZrSiO_4$), C (SiO_2 Cristobalite), A (Amorphous).
Peaks intensity: s (strong), m (medium), w (weak), vw (very weak).

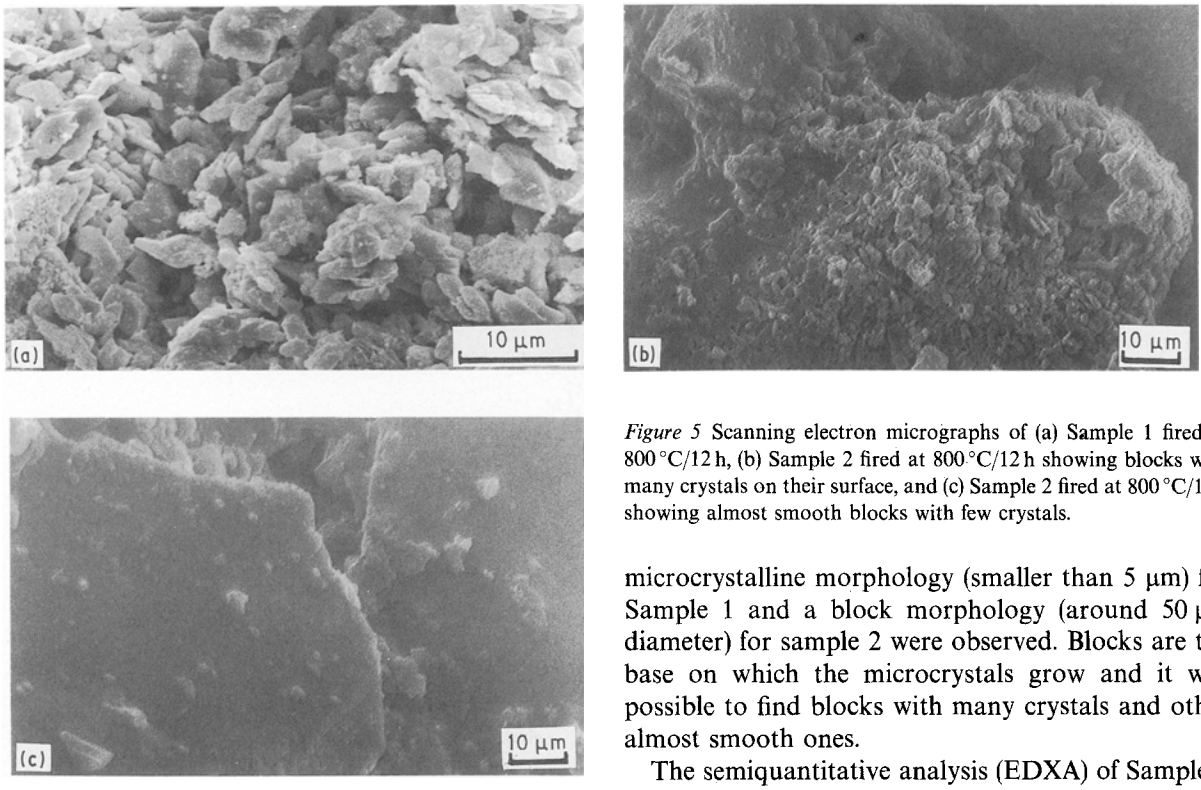

Figure 5 Scanning electron micrographs of (a) Sample 1 fired at 800 °C/12 h, (b) Sample 2 fired at 800 °C/12 h showing blocks with many crystals on their surface, and (c) Sample 2 fired at 800 °C/12 h showing almost smooth blocks with few crystals.

With increasing organic character of the sample, crystalline phases are detected at higher temperatures. However, the full development of the zircon phase is produced in a narrower range of temperature. In all samples the complete development of zircon at 800 °C can be observed. Likewise, although it is not possible to establish the temperature at which the phase transition ZrO_2(tetragonal) → ZrO_2(monoclinic), is produced, it seems clear that it occurs in all the narrower temperature ranges with increasing organic character of the samples.

In general, the following steps in the reaction mechanism are confirmed. The crystallization of metastable ZrO_2(tetragonal) is produced from an amorphous material, then the phase transformation ZrO_2-(tetragonal) → ZrO_2(monoclinic) takes place and later the reaction between ZrO_2(monoclinic) and amorphous silica occurs generating zircon together with a small amount of residual cristobalite.

3.4. Electron microscopy

Samples 1 and 2 fired at 800 °C/12 h (Fig. 5) were studied by scanning electron microscopy (SEM). A microcrystalline morphology (smaller than 5 μm) for Sample 1 and a block morphology (around 50 μm diameter) for sample 2 were observed. Blocks are the base on which the microcrystals grow and it was possible to find blocks with many crystals and other almost smooth ones.

The semiquantitative analysis (EDXA) of Sample 1 displayed lower vanadium contents than in Sample 2. In Sample 2, analysis of microcrystals showed a larger vanadium content than in the blocks. Similarly, a larger silicon content was detected in the smooth surface of blocks rather than in the microcrystals. This is consistent with the detection of cristobalite by X-ray diffraction.

4. Conclusions

The effect of zirconia precursors on the synthesis of zircon by the sol–gel process has been investigated and the following conclusions may be drawn.

1. The absence of Si–O–Zr vibration bands indicated no formation of a three-dimensional network containing zirconium together with silicon in polymeric gels. This was in agreement with the presence of bands between 645 and 600 cm^{-1}, attributed to ZrO_8 groups.

2. A higher organic character of zirconium oxide precursor was observed both at higher temperatures, for the formation of $ZrSiO_4$, and in narrower temperature ranges within which the whole development of the zircon phase was produced.

3. The main steps in the reaction mechanism for zircon formation were: crystallization of tetragonal ZrO_2 metastable; tetragonal ZrO_2 → monoclinic

ZrO_2 phase transformation; formation of zircon by reaction between monoclinic ZrO_2 and amorphous silica.

Acknowledgements

This work was supported by the DGICYT under project MAT88–0429. The authors thank the Instituto de Ceramica y Vidrio (C.S.I.C) for their cooperation in DTA, TG and DTG analysis.

References

1. G. MONROS, J. CARDA, P. ESCRIBANO and J. ALARCON, *J. Mater. Sci. Lett.* **9** (1990) 184–186.
2. G. MONROS, J. CARDA, M. A. TENA, P. ESCRIBANO, and J. ALARCON, *ibid.* **9** (1990) 484.
3. Y. MURASE, E. KATO and K. DAIMON, *J. Amer. Ceram. Soc.* **69**(2) (1986) 86.
4. V. S. NAGARAJAN and K. J. RAO, *J. Mater. Sci.* **24** (1989) 2140.
5. M. NOGAMI and M. TOMOZAWA, *J. Amer. Ceram. Soc.* **69**(2) (1986) 99.
6. L. J. BELLAMI, in "The Infra-red Spectra of Complex molecules" (Wiley, New York, 1958) pp. 384–93.
7. A. SAMDI, T. GROLLIER, B. DURAND and E. ROUBIN, *Ann. Chim. Fr.* **13** (1988) 171.

Received 26 March
and accepted 20 December 1990